Chapter 11. Ommatidial chirality in PCP mutants, the *ft/ds/fj* cassette and pre-cluster rotation.

The fine-scale patterning of most imaginal discs takes place during pupal metamorphosis. However, if ommatidial pre-clusters were recruited inwards from the boundary of a ring of Wg expressing cells, like the D/V margin of the wing blade, then radial stacking flaws would develop with disrupted ommatidial packing. Instead, the eye twin-field is initiated by three ommatidia in the early larval stage, which sets the P limit of the eye and the equator (Fig. 15). Subsequent ommatidia align against this initial column and extend further from the equator, with the perimeter of the eye twin-field delimited by the last pre-cluster to be recruited in successive columns, see above **10**. Thus, mutants that affect furrow progression may generate rough eyes, with distorted corneal lenses and altered twin-field boundaries. Indeed, rough-eyed phenotypes are associated with some mutant alleles of *hh*, *N*, *wg*, and many other, morphogenetic functions. In particular, the corneal lenses are flattened and reduced in *glass* (*gl*) and *wingless*^{Glazed} (*wg*^{Gla}) mutants, consistent with defective secretion of the cuticular lens.

In this context, the Bar (B) mutant phenotypes are consistent with incomplete pre-cluster rotation and delayed cell-cycle progression. The mutant *B* alleles form a phenotypic series, with tandem duplications of the homoebox TFs, *B-H1* and *B-H2* [1 2]. Mild *B* alleles, cause equatorial defects that become more severe from P > A. The ommatidial columns become progressively curved, with incremental equatorial > polar delays and premature termination of the twin-field boundaries, (Fig. 16).

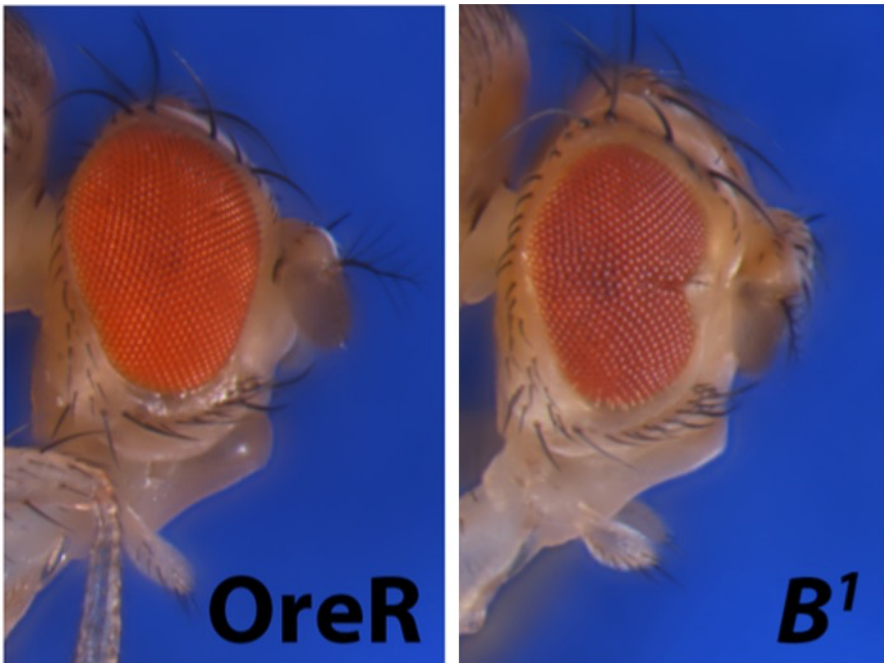

Fig. 16. Tessellated ommatidial array. Wild-type (Oregon R strain) and *Bar*^{1} mutant eyes, from FlyBase images.

In strong *B* alleles the eyes are reduced to a vertical bar of about 70 ommatidia [3]. The *B-H1* and *B-H2* cognate genes also specify the fate of the last R-cell pair (R1 + R6) to be recruited. Notably, ectopic expression of *UAS-B-H1*, driven by *sevenless-Gal4*, supresses expression of the *rough* TF (in R3 and R4) and activates expression of B-H2 in the R1, R6 and R7 photoreceptors; which transform to primary pigment cells [4]. Deletion of the cognate *B-H1* + *BH2* genes results in ectopic expression of *dpp* [2]. Intriguingly, the classical *bar-3* mutation maps to neither of the *B-H* genes but is associated with a 1.9 kb intronic deletion within *hh* (*hh*^{bar3}) [5].

By contrast, the PCP mutants show more specific stacking defects, with the direction of pre-cluster rotation being random to either side of the equator. These mutations give rough-eyed arrays of distorted lenses, with mixed ommatidial chirality. The onset of pre-cluster rotation may be delayed, with pre-clusters failing to turn through a full 90^{o} before differentiation [6 7]. In this respect, *pk*^{sple} mutants are atypical in that they show a uniform hexagonal array with mixed chirality [8]. Ommatidial rotation appears not be delayed in *pk*^{sple} mutants, but can be either clockwise, or anticlockwise; with the adult ommatidia showing chiral

reflections around either the polar, or the equatorial, axis [6]. By contrast, *pk*^{pk} mutants have wild-type eyes, while the double-mutant, *pk*$^{pk\text{-}sple}$, alleles give a rough-eye phenotype, similar to that of other PCP mutants. In general, in somatic mosaics of PCP mutant cells, ommatidial chirality is determined by the genotype of the R3 and R4 precursors, with the cell closest to the equator becoming R3, reviewed in [9]. In *pk*$^{pk\text{-}sple}$ mosaics, however, the genotype of both R2 and R3 cells affects the chirality of mosaic ommatidia [6]. Thus, the Pk protein isoforms may affect R cell recruitment (and pre-cluster rotation) along both the polar and equatorial axes. In wild-type imaginal discs, the Fz, Dsh, Vang, Pk and Stan proteins are asymmetrically expressed in R3 and R4 cells, with preferential localisation to the lateral R cell boundaries [9 10]. By implication, the coordinated deployment of core PCP functions may be regulated by asymmetrical partitioning during terminal differentiation. Taken together, these studies confirm that furrow progression determines both R cell fate and ommatidial chirality.

While the PCP mutations modify pre-cluster rotation, the cytoskeletal remodelling of R cells is not completely blocked. During normal development, contractile actin microfilaments are coupled across the extracellular matrix between neighbouring cells, with cell adhesion maintained by E-Cadherin (aka: shotgun, shg) and Stan. In the initial 5 cell pre-cluster, R5 and R4 lie on the polar flanks of R8, while R2 and R3 are equatorial, Fig. 14. Thus, Wg flux from the posterior D and V margins of the eye twin-field may drive mirror-image recruitment of ommatidial arrays. These observations are consistent with microtubule remodelling initiated via the Wg/Fz signalling pathway, coupled with contractile sliding of actomyosin filaments. Thus, active trafficking through lateral cell interfaces may generate a polarised morphogen flux and transmit vectorial information, without the requirement for an extracellular diffusion gradient. Meanwhile, differential transcriptional responses may be imposed by the extended TUs of PCP gene functions during furrow progression, including *pk*^{pk} (74 kb), *pk*^{sple} (36 kb), *fz* (94 kb), *stan* (48 kb) and *dgo* (3.8 kb). In the case of *pk*, the expression of the mutually antagonistic Pk^{pk} and Pk^{sple} isoforms may influence the onset of rotation. However, the critical balance may well be between the activities of the Pk isoforms and Dgo, transcribed from its much shorter TU. Whatever the detailed mechanisms, the sequential localisation of protein activities must be keyed to the progression of the advancing furrow.

During these cellular rearrangements, the actomyosin contractions that drive ommatidial rotation are triggered by the *nemo* (*nmo*) kinase. In *nmo* mutants, the normal 90^{o} rotation of ommatidial pre-clusters is arrested at 45^{o} [11 12]. Nmo regulates F-actin contractile sliding via MyoII and E-cadherin [13 14 15]. Transmembrane anchoring of the cortical actin cytoskeleton to the extracellular matrix is modulated, via phosphorylation of a β-catenin/E-Cad complex and Vang, with the Stan cadherin coupled to SNX27, Sorting Nexin 27, [15 16]. In this context, Pk is an additional substrate of the Nmo kinase, with the Pk^{pk}/Pk^{sple} balance altered in *nmo* mutants, and rapid degradation of Pk^{Pk} [17], again with the *caveat* that a critical balance might include the *pk* cognate gene *esn*. Indeed, Esn protein-protein interactions (PPIs) via Stan may be linked to Fz and Par-3 [18 19 20]. Thus, while pre-cluster rotation may be driven primarily by coupled actomyosin contractions, the co-ordinate regulation of microtubule remodelling is also required during the cell-shape changes associated with furrow progression. The progressive recruitment of ommatidial pre-clusters may be limited by the polar gradient of the Fj kinase, with indirect effects on the Hh, Dpp and Wg signalling pathways. In addition to regulating heterotypic binding of the Ft and Ds cadherins, the Fj kinase interacts with Wnt4, Calmodulin, Myo61F and Klp61F, affecting both microtubule assembly and cortical F-actin anchoring to the extracellular matrix [21]. Taken together, these results indicate that the core PCP functions are deployed during the asymmetric partitioning of morphogen and TF activities, coupled to cytoskeletal remodelling and the allocation of alternative cell fates.

Summary:

The initial column of three ommatidial pre-clusters defines the P margin of the eye and sets an equatorial AMS. As subsequent columns of ommatidia extend from the equator, its twin-field boundaries are delimited by the last pre-cluster to be recruited. Thus, R cell fate and the shape of the composite eye structure are both keyed to the topography of the advancing morphogenetic furrow, with sequential deployment of PCP gene functions. The ommatidial pre-clusters rotate in separate, 45^{o} steps, with a second wave of cell division, as the polar pre-cluster axis re-aligns with the equator. At this stage, the R7 cell has been displaced below R8: consistent with a closed-loop cascade of morphogenetic interactions. Ommatidial chirality, R-cell fate and the hexagonal packing of corneal

lenses are all disrupted if pre-clusters fail to complete their full 90º rotation. Asymmetric partitioning of morphogens between presumptive R cells may allocate alternative, M-twin, fates. Meanwhile, the *ft/ds/fj* cassette may regulate cadherin anchoring of the actin cytoskeleton to the extracellular matrix, during imaginal disc growth and terminal PCP signalling.

References:

1. Muller, H. J., Prokofyeva-Belgovskaya, A. A. & Kossikov, K. V. Unequal crossing-over in the Bar mutant as a result of duplication of a minute chromosome section. *Dokl. Akad. Nauk Soiuza Sov. Sotsialisticheskikh Resp.* **1**, 87–88 (1936).
2. Kang, J., Yeom, E., Lim, J. & Choi, K. W. Bar Represses dPax2 and Decapentaplegic to Regulate Cell Fate and Morphogenetic Cell Death in Drosophila Eye. *PLoS ONE* **9**, e88171 (2014).
3. Lindsley, D. L & Zimm, G. G. *The Genome of Drosophila Melanogaster.* (Academic press, 1992).
4. Hayashi, T., Kojima, T. & Saigo, K. Specification of primary pigment cell and outer photoreceptor fates by BarH1homeobox gene in the developing Drosophila Eye. *Dev. Biol.* **200**, 131–145 (1998).
5. Rogers, E. M. *et al.* Pointed regulates an eye-specific transcriptional enhancer in the Drosophila hedgehog gene, which is required for the movement of the morphogenetic furrow. *Development* **132**, 4833 (2005).
6. Gubb, D. Cellular polarity, mitotic synchrony and axes of symmetry during growth. Where does the information come from? *Int. J. Dev. Biol.* **42**, 369–377 (1998).
7. Strutt, D., Johnson, R., Cooper, K. & Bray, S. Asymmetric localization of frizzled and the determination of notch-dependent cell fate in the Drosophila eye. *Curr. Biol.* **12**, 813–824 (2002).
8. Choi, K. W., Mozer, B. & Benzer, S. Independent determination of symmetry and polarity in the Drosophila eye. *Proc. Natl. Acad. Sci. U. S. A.* **93**, 5737–5741 (1996).
9. Maung, S. M. Planar cell polarity in Drosophila. *Organogenesis* **7**, 165–179 (2011).
10. Strutt, D., Johnson, R., Cooper, K. & Bray, S. Asymmetric localization of frizzled and the determination of notch-dependent cell fate in the Drosophila eye. *Curr. Biol.* **12**, 813–824 (2002).
11. Choi, K. W. & Benzer, S. Rotation of photoreceptor clusters in the developing Drosophila eye requires the nemo gene. *Cell* **78**, 125–136 (1994).
12. Firth, L. C., Bhattacharya, A. & Baker, N. E. Cell cycle arrest by a gradient of Dpp signaling during Drosophila eye development. *BMC Dev. Biol.* **10**, 28 (2010).
13. Fiehler, R. W. & Wolff, T. Drosophila Myosin II, Zipper, is essential for ommatidial rotation. *Dev. Biol.* **310**, 348–362 (2007).
14. Fiehler, R. W. & Wolff, T. Nemo is required in a subset of photoreceptors to regulate the speed of ommatidial rotation. *Dev. Biol.* **313**, 533–544 (2008).
15. Mirkovic, I. *et al.* Nemo kinase phosphorylates ?-catenin to promote ommatidial rotation and connects core PCP factors to E-cadherin-?-catenin. *Nat. Struct. Mol. Biol.* **18**, 665–672 (2011).
16. Strutt, H. *et al.* Retromer controls planar polarity protein levels and asymmetric localization at intercellular junctions. *Curr. Biol.* **29**, 484-491.e6 (2019).
17. Collu, G. *et al.* Prickle is phosphorylated by Nemo and targeted for degradation to maintain Prickle/Spiny-Legs isoform balance during planar cell polarity establishment. PLoS Genetics **14**, 1007391 (2018).
18. Wasserscheid, I., Thomas, U. & Knust, E. Isoform-specific interaction of Flamingo/Starry Night with excess Bazooka affects planar cell polarity in the Drosophila wing. *Dev. Dyn.* **236**, 1064–1071 (2007).
19. Chen, W.-S. *et al.* Asymmetric homotypic interactions of the atypical cadherin flamingo mediate intercellular polarity signaling. *Cell* **133**, 1093–1105 (2008).
20. Matsubara, D., Horiuchi, S. Y., Shimono, K., Usui, T. & Uemura, T. The seven-pass transmembrane cadherin Flamingo controls dendritic self-avoidance via its binding to a LIM domain protein, Espinas, in Drosophila sensory neurons. *Genes Dev.* **25**, 1982–1996 (2011).
21. Kwon, Y. *et al.* The Hippo signaling pathway interactome. *Science* **342**, 737–740 (2013).